

**ROLE OF SOME PYRAZOL-5-ONE DERIVATIVES AS CORROSION
INHIBITORS FOR 316L STAINLESS STEEL in 1 M HCl**

A.S. Fouda^a, G.Y. El-Ewady^a, A.M.El-Desoky^b, and S.Fathy^a

^aDepartment of Chemistry, Faculty of Science, El-Mansoura University, El-Mansoura-
35516, Egypt, Email: asfouda@mans.edu.eg

^bChemistry Department, High Institute of Engineering & Technolog (New Damietta) ,
Egypt

(Received : 7/12/2011)

ABSTRACT

The effect of novel corrosion inhibitors, pyrazolone derivatives namely, (Z)-3-methyl-4-(2-m-tolylhydrazono)-1H-pyrazol-5(4H)-one compound (A), (Z)-4-(2-(3-methoxyphenyl)hydrazono)-3-methyl-1H-pyrazol-5(4H)-one compound (B) and (Z)-3-methyl-4-(2-(3-nitrophenyl) hydrazono) -1H-pyrazol-5(4H)-one compound (C) on the corrosion of 316L stainless steel (SS) in 1 M HCl has been investigated by using weight loss, potentiodynamic polarization, electrochemical impedance spectroscopy (EIS) and electrical frequency modulation (EFM) techniques. Polarization data clearly indicated that the pyrazol-5-one derivatives behave as mixed type inhibitors. The effect of temperature on corrosion inhibition has been studied and the thermodynamic activation and adsorption parameters were calculated and discussed. EIS was used to investigate the mechanism of corrosion inhibition. EFM can be used as a rapid and non destructive technique for the corrosion rate measurements without prior knowledge of Tafel constants. The adsorption of the used compounds on 316L SS was found to obey Temkin's adsorption isotherm.

Keywords 316L SS; HCl; EFM; EIS; pyrazol-5-one derivatives

INTRODUCTION

Austenitic stainless steel (SS) are widely used in many applications where high corrosion resistance is required, such as in the petrochemical and pharmaceutical industries, industrial power generation and desalination plants. However, certain factors in the handling or manufacturing of these alloys can make them susceptible to localized corrosion and affect their performance. Cleaning and pickling remove foreign materials and promote stability, achieving a uniform surface that is resistant to localized corrosion. SS passivation favors corrosion resistance by forming a protective oxide film [C.D. Dillon(1994)].

The selection of appropriate inhibitors mainly depends on the type of acid, its concentration and temperature. The presence of dissolved organic and/ or inorganic substances and, of course on the type of metallic material exposed to the action of the acidic solution [W.P.Wang et al,(1994); P.Q.Zhang et al,(1993) and A.Atrems et al,(1997)]. Also, cost, toxicity, and availability are important factors in the selection and utilization of these inhibitors. A number of studies have recently appeared in the literature [Fadda et al,(2003); R.W.Bosch et al,(2001); D. A. Jones et al,(1983); M. Kendig et al,(2002); F. Mansfeld et al,(1982); F. Mansfeld et al,(1990); E. McCafferty et al,(1972); R.W.Bosch et al,(2001); K. F. Khaled et al,(2008); K. F. Khaled et al,(2008); W. Huilong et al,(2002); M. T. Said et al,(2003); Atia et al,(2003) and S. Tamilselvi et al,(2003)] on the topic of the corrosion inhibition of 316L SS in acidic media by organic compounds.

The corrosion inhibition of 316L SS becomes of such interest to do because of its widely used as a constructional material in many industries and this is due to its excellent mechanical properties and low cost. So, we try to study its corrosion inhibition in HCl using some new pyrazol-5-one derivatives by different techniques.

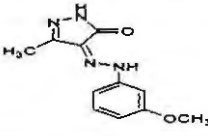
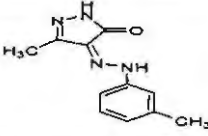
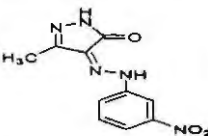
EXPERIMENTAL

The 316L SS used in this study had the chemical composition C 0.02 %, Mn 1%, P 0.054%, S 0.02%, Si 1%, Cr 16%, Ni 11%, Mo 3% Cu 0.2% and Fe balance.

Analar grade 37 % HCl and bidistilled water were used to prepare all the solutions. All the experiments were performed at 25 °C.

The inhibitors were synthesized in the laboratory according to a previously described experimental procedure [D. A. Jones et al,(1983)] purified and characterized by NMR and IR spectroscopes and elemental analysis before use. The structure formula of the inhibitors examined is given in **Table (1)**.

Table (1) The chemical structure of the investigated pyrazol-5-one derivatives

Comp.	Structure	Name	Formula & Molecular Weight
(A)		(Z)-4-(2-(3-methoxyphenyl)hydrazono)-3-ethyl-1H-pyrazol-5(4H)-one	C ₁₁ H ₁₂ N ₄ O ₂ 232.24
(B)		(Z)-3-methyl-4-(2-m-tolyl hydrazono)-1H-pyrazol-5(4H)-one	C ₁₁ H ₁₂ N ₄ O 216.24
(C)		(Z)-3-methyl-4-(2-(3-nitrophenyl)hydrazono)-1H-pyrazol-5(4H)-one	C ₁₀ H ₉ N ₅ O ₃ 247.21

Weight loss measurements were performed on 316L SS coupons with dimensions 2 x 2 x 0.2 cm in 1 M HCl solution with different concentrations of the inhibitor. The coupons were abraded with a series of emery papers of different grit sizes up to 1200, dried and weighted, and then suspended in 100 ml solution of HCl without and with different concentrations of the studied inhibitors for exposure period of 3 hours at the temperature range from 25°C to 55°C. At the end of tests, the coupons were rinsed with distilled water, degreased with acetone, washed thoroughly again with bidistilled water, dried by filter papers, and weighed again. Experiments were carried out in triplicate to get good reproducibility.

Electrochemical experiments used 316L SS specimen of the same composition was mounted in glass rod with an exposed area of 1cm². An epoxy resin was used to fill the space between glass rod and 316L SS electrode. The electrochemical measurements (potentiodynamic polarization, EIS and EFM techniques) were performed in a conventional three-electrode glass cell with 316L SS specimen as working electrode, platinum sheet as counter electrode, and a saturated calomel electrode (SCE) as reference electrode. Prior to each experiment, the electrode was treated as in weight loss measurements. The electrode potential was allowed to stabilize to 30 min before starting the measurements. For potentiodynamic polarization the electrode potential automatically changed from -600 to +400 mV versus open circuit potential (E_{OCP}) with a scan rate of 5 mVs⁻¹. For electrochemical impedance spectroscopy (EIS) measurements experiments were conducted in the frequency range of 100 kHz to 10 mHz at open circuit potential (OCP). The amplitude was 5 mV. For electrochemical frequency modulation (EFM) measurements experiments were carried out using two frequencies 2 and 5 Hz. The base frequency was 1Hz with 32 cycles, so the waveform repeats after 1s. A perturbation signal with amplitude of 10 mV was used. The choice for the frequencies of 2 and 5 Hz was based on three principles [Gamry (2003)].

Electrochemical measurements were performed with a Potentiostat/Galvanostat/ZRA (Gamry PCI 300/4) and a personal computer with DC105 software for dc corrosion measurements, EIS300 software for EIS measurements and EFM140 software for EFM measurements. Echem Analyst software 5.1 was used for plotting, graphing and fitting data. The measurements were carried out

RESULTS AND DISCUSSION

Weight loss measurements

To elucidate the mechanism of inhibition and to determine the thermodynamic parameters of the corrosion process, weight loss measurements were performed at 25 to 55 °C. Weight-loss of 316L SS was determined, at various time intervals in the absence and presence of different concentrations of pyrazol-5-one derivatives (A-C). The obtained weight loss-time curves are represented in **Figure (1)** for inhibitor (A), the most effective one. Similar curves were obtained for other inhibitors (not shown).

The curves obtained in the presence of inhibitors fall significantly below that of free acid. In all cases, the increase in the inhibitor concentration was accompanied by a decrease in weight-loss and an increase in the percentage inhibition. These results led to the conclusion that, these inhibitors are fairly efficient inhibitors for 316L SS dissolution in HCl solution. The degree of surface coverage (θ) and the inhibition efficiency ($\% \eta$) were calculated using the following equation:

$$\% \eta = \theta \times 100 = [1 - (\Delta W_{inh} / \Delta W_{free})] \times 100 \quad (1)$$

where ΔW_{inh} and ΔW_{free} are the weight loss per unit area in presence and absence of the inhibitor, respectively.

The values $\% \eta$ obtained for pyrazol-5-one derivatives at different concentrations and at 25°C are summarized in **Table (2)**.

Careful inspection of these results showed that, at the same inhibitor concentration, the order of inhibition efficiency was as follows: $A > B > C$

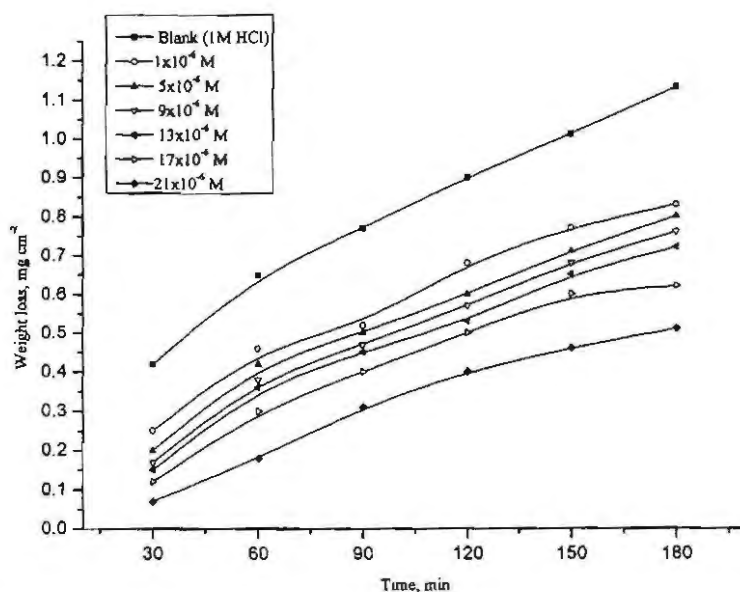


Figure (1) Weight loss-time curves for the dissolution of 316L SS in the absence and presence of different concentrations of compound (A) in HCl at 25°C

Table (2) Inhibition efficiency (% η) of corrosion of 316L SS in 1 M HCl in the presence of different concentrations of pyrazol-5-one derivatives at 25 °C and at 90 min immersion

Conc., M	inhibition efficiency (% η)		
	A	B	C
1x10 ⁻⁶	29	26	20
5x10 ⁻⁶	35	31	28
9x10 ⁻⁶	41	38	35
13x10 ⁻⁶	44	41	38
17x10 ⁻⁶	54	49	46
21x10 ⁻⁶	72	60	54

Adsorption isotherm behavior

The nature of corrosion inhibition has been deduced in terms of the adsorption characteristics of the inhibitors. Metal surface in aqueous solution is always covered with adsorbed water dipoles. Therefore, adsorption of inhibitor molecules from aqueous solution is a quasi substitution process. The degree of surface coverage (θ) for different concentration of the inhibitors has been evaluated from weight loss measurements. The data were tested graphically by fitting to various isotherms. A straight line with correlation coefficient nearly equal to 1.0 ($R^2 > 0.9$) was obtained on plotting (θ) against $\ln C$ suggesting adsorption of pyrazol-5-one derivatives on SS surface followed Temkin adsorption isotherm model Fig. (2). According to this isotherm, the surface coverage is related to inhibitor concentration by:

$$KC = \exp(-2a\theta) \quad (2)$$

where "a" is the molecular interaction parameter and K is the equilibrium constant of the adsorption process.

The free energy of adsorption ΔG°_{ads} was calculated from the following equation:

$$\Delta G^\circ_{ads} = -RT \ln(55.5 K) \quad (3)$$

where 55.5 is the concentration of water in solution in mol l⁻¹, R is the universal gas constant and T is the absolute temperature.

The standard free energy for adsorption was calculated using Eq. (3) where one molecule of water is replaced by one molecule of inhibitor [I.O'Mbockris et al,(1964)]. The values of ΔG°_{ads} and K are given in Table (3). The negative sign of ΔG°_{ads} indicates that the adsorption of these inhibitors at SS surface is a spontaneous process. Generally, the magnitude of ΔG°_{ads} around -20 kJ mol⁻¹ or less negative indicates electrostatic interaction between inhibitor and the charged metal surface (i.e. physisorption). Those around -40 kJ mol⁻¹ or more negative indicative of charge sharing or transferring from the inhibitor molecules to the metal surface to form a co-ordinate type of bond (i.e. chemisorptions) [F.M.Donahuce et al,(1965) and E.Kamis et al,(1991)]. In the present work, the calculated values of free energy of these inhibitors Table (4) are -20 kJ mol⁻¹ or less which indicated that adsorption of these inhibitors on SS surface takes place via physisorption. Large values of K_{ads} mean better inhibition efficiency of the inhibitors, i.e., strong electrical interaction between the double-layer existing at the phase boundary and the adsorbing inhibitor molecules (which is in our case). Small values of K_{ads} , however, reveal that such interactions between adsorbing inhibitor molecules and the metal surface are weaker, indicating that the inhibitor molecules are easily removable by the solvent molecules from the metal surface [M.A.Amin et al,(2009)].

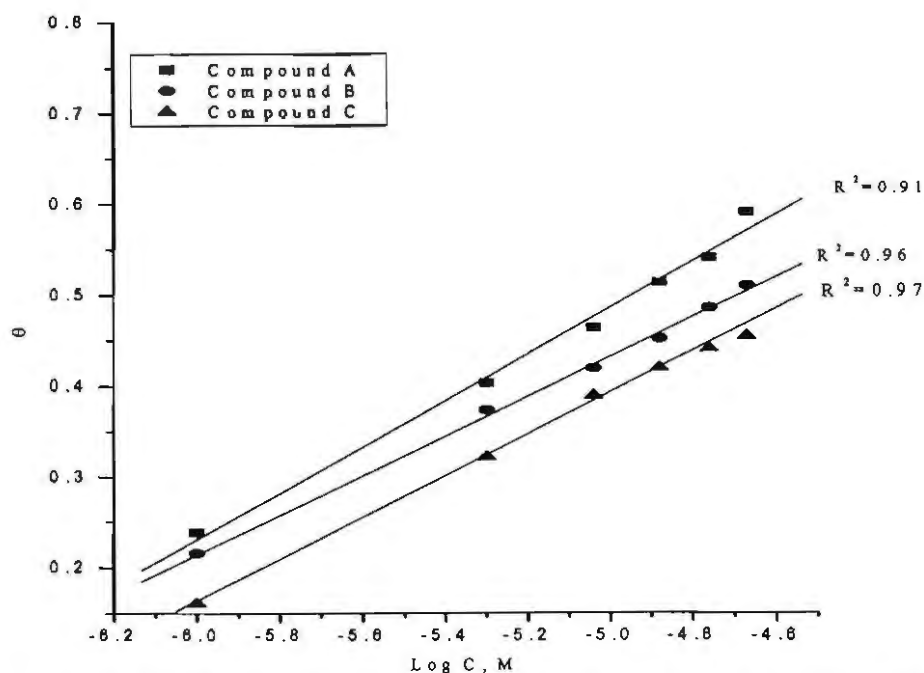


Figure (2) Temkin adsorption isotherm plotted as θ vs. $\log C$ of the investigated inhibitors for corrosion of 316L SS in 1 M HCl solution from weight loss method at 25°C

Table (3) Equilibrium constant (K_{ads}), adsorption free energy (ΔG°_{ads}) for the adsorption of inhibitors on 316L SS in 1 M HCl from weight loss method at 25°C

Inhibitor	Temkin adsorption isotherm	
	$K_{ads} \times 10^{-4} M^{-1}$	$-\Delta G^{\circ}_{ads} kJ mol^{-1}$
A	1000	21.7
B	178	19.8
C	148	19.5

Effect of Temperature

The temperature is the accelerating factor in most of chemical reactions. It increases the energy of the reacted species, as a result, chemical reaction get much faster. The corrosion reaction is a chemical reaction in which the Fe atoms at the metal surface react with the negatively charged anions (OH⁻, SO₄²⁻, Cl⁻, etc.). Hence, increasing temperature of the environment increases the activation energy of the Fe atoms at the metal surface and accelerates the corrosion process of SS in the acidic media.

The effect of temperature on the corrosion inhibition efficiencies of the tested inhibitors was determined in the absence and presence of different inhibitors at concentrations of 1×10^{-6} - 21×10^{-6} M at 25 – 55 °C. In examining the effect of temperature on the corrosion of SS in presence of studied inhibitors in 1 M HCl solution, Arrhenius Eq. (4) was used [E.E.Oguzie et al,(2006)].

Arrhenius – type plot:

$$k = A \exp (-E_a^* / RT) \quad (4)$$

where E_a^* is the apparent activation energy and A is the frequency factor.

Plots of $\log k$ (corrosion rate) against $1/T$ Fig. (3) for 316L SS in 1 M HCl, gave straight lines with slope of $-E_a^*/2.303R$ at which the activation energies were calculated and represented in Table (4).

Activation parameters for corrosion of 316L SS were calculated from transition state- type equation:

$$k = RT / Nh \exp (\Delta S^* / R) \exp (-\Delta H^* / RT) \quad (5)$$

The relation between $\log k / T$ vs. $1 / T$ gives straight lines Fig. (4), from their slopes and intercepts, ΔH^* and ΔS^* can be calculated and their values are represented in Table (4).

The results of Table (4) revealed that, the presence of inhibitors increases the activation energies of 316L SS indicating strong adsorption of the inhibitor molecules on the metal surface and the presence of these additives induces energy barrier for the corrosion reaction and this barrier increases with increasing the inhibitor concentrations. Higher activation energy means lower reaction rate and the opposite is true. The increase in activation energy with inhibitor concentration is often interpreted by physical adsorption with the formation of an adsorptive film of an electrostatic character [A.Popova et al,(2003)]. Values of ΔH^* are positive. This indicates that the corrosion process is an endothermic one. The entropy of activation is large and negative. This implies that the activated complex represents association rather than dissociation step, indicating that a decrease in disorder takes place, from reactants to the activated complex [A.S.Fouda et al,(2010)].

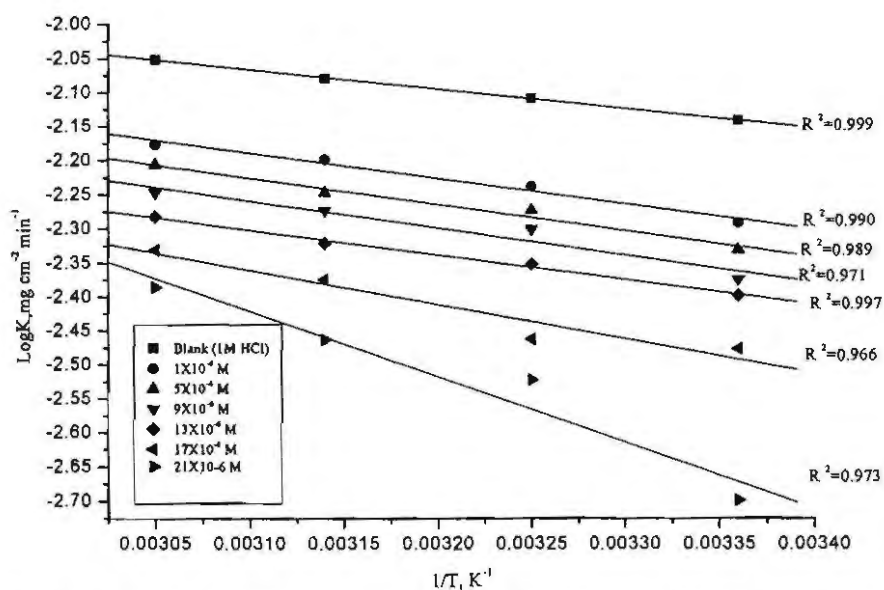


Figure (3) Arrhenius plots ($\log k$ vs. $1/T$) for the corrosion of 316L SS in 1 M HCl in the absence and presence of different concentrations of inhibitor (A)

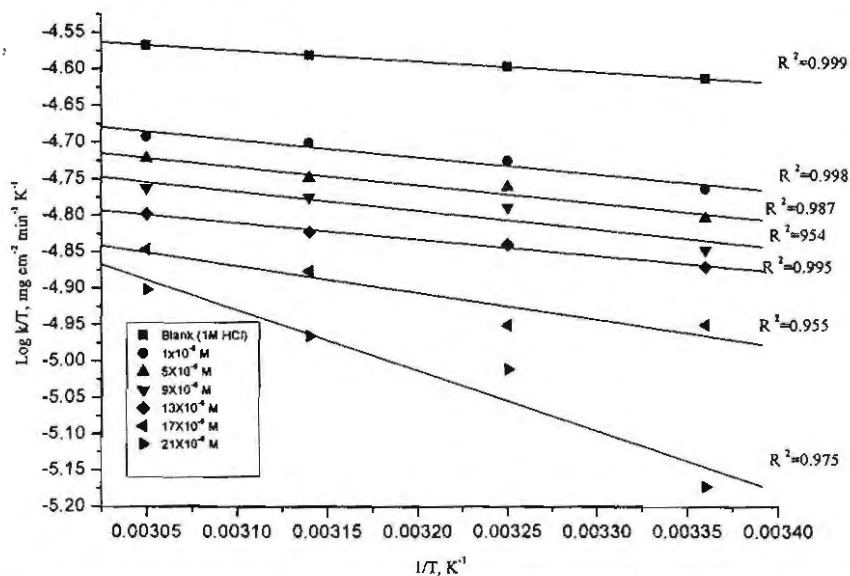


Figure (4) Plots of ($\log k / T$) vs. $1/T$ for the corrosion of 316L SS in 1 M HCl in the absence and presence of different concentrations of inhibitor (A)

Table (4) Thermodynamic activation parameters for the dissolution of 316L SS in 1 M HCl in the absence and presence of different concentration of investigated inhibitors

Inhibitor	Conc. M	E_a^* kJ mol ⁻¹	ΔH^* kJ mol ⁻¹	$-\Delta S^*$ J mol ⁻¹ K ⁻¹
Blank	1 M HCl	5.52	2.97	275.8
A	1x10 ⁻⁶	7.15	4.59	273.9
	5X10 ⁻⁶	7.38	4.82	273.2
	9X10 ⁻⁶	7.62	5.07	273.0
	13X10 ⁻⁶	7.14	6.41	270.8
	17X10 ⁻⁶	9.66	7.11	268.6
	21x10 ⁻⁶	18.47	15.94	242.5
B	1x10 ⁻⁶	7.98	5.45	269.92
	5X10 ⁻⁶	7.31	4.79	269.92
	9X10 ⁻⁶	8.72	6.20	268.98
	13X10 ⁻⁶	7.96	5.42	260.02
	17X10 ⁻⁶	8.97	6.44	252.91
	21x10 ⁻⁶	11.55	13.70	235.90
C	1x10 ⁻⁶	7.22	4.67	272.1
	5X10 ⁻⁶	7.21	4.66	272.9
	9X10 ⁻⁶	8.06	5.50	270.8
	13X10 ⁻⁶	7.62	5.07	269.7
	17X10 ⁻⁶	9.12	6.57	268.1
	21x10 ⁻⁶	11.75	8.02	265.2

Electrochemical measurement**Potentiodynamic polarization measurements**

Polarization measurements were carried out to obtain Tafel plots in the absence and presence of various concentrations of the inhibitors. Figure (5) shows the polarization curves in the absence and presence of inhibitor (A). Similar curves were obtained for other inhibitors (not shown). It is observed that the current density of the anodic and cathodic branch is displaced towards lower values. This displacement is more evident with the increase in concentration of the inhibitors when compared to the blank material. The electrochemical parameters of corrosion such as corrosion current density j_{corr} , corrosion potential E_{corr} , corrosion rate C.R., anodic Tafel constants β_a , cathodic Tafel constants β_c and inhibition efficiency η_{Tafel} (%) are given in Table (5). The inhibition efficiency (η_{Tafel} %) was calculated from polarization curves as follows [M. Kendig et al, (2002)]:

$$\eta_{Tafel}\% = [1 - (j_{corr} / j_{corr}^0)] \times 100 \quad (6)$$

where j_{corr}° and j_{corr} correspond to uninhibited and inhibited corrosion current densities, respectively.

It appears that inhibition occurred by a blocking mechanism on the available metal spaces [K.C.Emeregul et al,(2006)]. The corrosion potential displayed small change in the range ± 14 mV around the corrosion potential of - 400 mV. These results indicated that the presence of inhibitors affect both SS dissolution and hydrogen evolution; consequently these inhibitors can be classified as mixed corrosion inhibitors.

According to the results in Table (5) the order of the inhibition efficiency was as follows: A > B > C. It is important to note that there exists a difference in inhibition efficiency determined by weight loss and polarization methods. This may be, due to the longer time taken in case of weight loss (3 h) than in case of polarization method (30 min after reaching OCP).

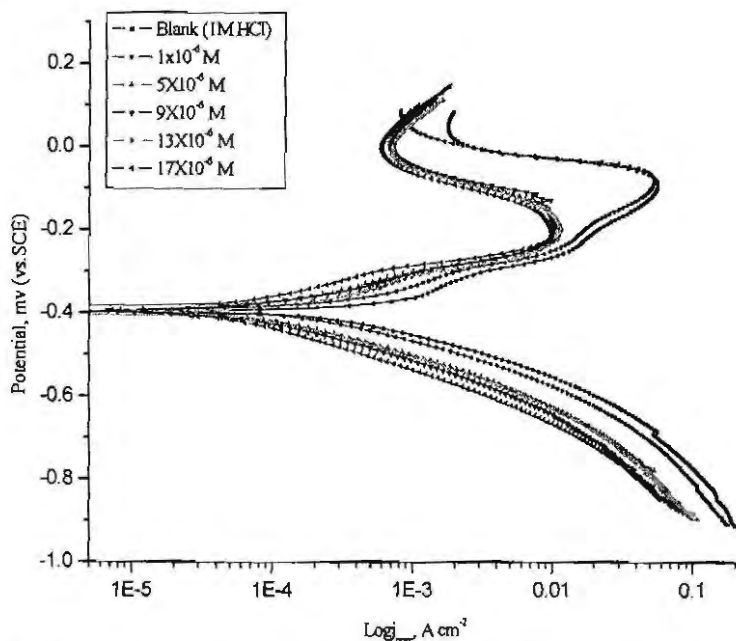


Figure (5) Potentiodynamic polarization curves for the dissolution of 316L SS in 1 M HCl in the absence and presence of different concentrations of inhibitor A at 25°C

Table (5) Electrochemical kinetic parameters obtained from potentiodynamic polarization technique for the corrosion of 316L SS in 1 M HCl at different concentrations of investigated inhibitors at 25 °C

Inhibitor	Conc. M	$-E_{corr}$ mV, vs. SCE	$J_{corr} \times 10^{-4}$ mA cm ⁻²	β_c mV dec ⁻¹	β_a mV dec ⁻¹	R_p Ω cm ²	θ	% η	CR mmy ⁻¹
Blank	1	397	36.2	109	94	313	-----	-----	161.3
A	1X10 ⁻⁶	394	20.1	107	86	546	0.400	40.0	89.83
	5x10 ⁻⁶	393	8.4	110	79	1260	0.770	77.0	37.64
	9X10 ⁻⁶	397	7.2	108	76	1426	0.800	80.0	31.92
	13X10 ⁻⁶	400	4.1	86	62	2023	0.900	90.0	17.74
	17X10 ⁻⁶	389	2.0	93	57	4068	0.960	96.0	8.002
B	1X10 ⁻⁶	402	31.9	106	98	365	0.125	12.0	142.4
	5x10 ⁻⁶	399	20.4	110	77	511	0.430	43.0	91.14
	9X10 ⁻⁶	414	8.6	97	93	1271	0.770	77.0	38.26
	13X10 ⁻⁶	407	0.67	92	114	1735	0.810	81.0	30.06
	17X10 ⁻⁶	365	0.21	105	78	3908	0.940	94.0	9.15
C	1X10 ⁻⁶	400	3.27	108	93	351	0.110	11.0	145.9
	5x10 ⁻⁶	391	21.9	99	83	475	0.400	40.0	97.74
	9X10 ⁻⁶	388	19.9	110	71	958	0.470	47.0	88.67
	13X10 ⁻⁶	382	16.2	112	73	1255	0.550	55.0	72.34
	17X10 ⁻⁶	388	12.9	97	76	1521	0.640	64.0	57.63

Electrochemical impedance spectroscopy (EIS)

EIS measurements were carried out at 25°C in acid solution with and without inhibitors. Fig. (6) shows the typical EIS diagrams obtained in 1 M HCl with and without inhibitor (A). The charge transfer resistance (R_{ct}) is calculated from the difference in impedance at lower and higher frequencies. The double layer capacitance (C_{dl}) and the frequency at which the imaginary component of impedance is maximal ($-Z_{max}$) are found as follow:

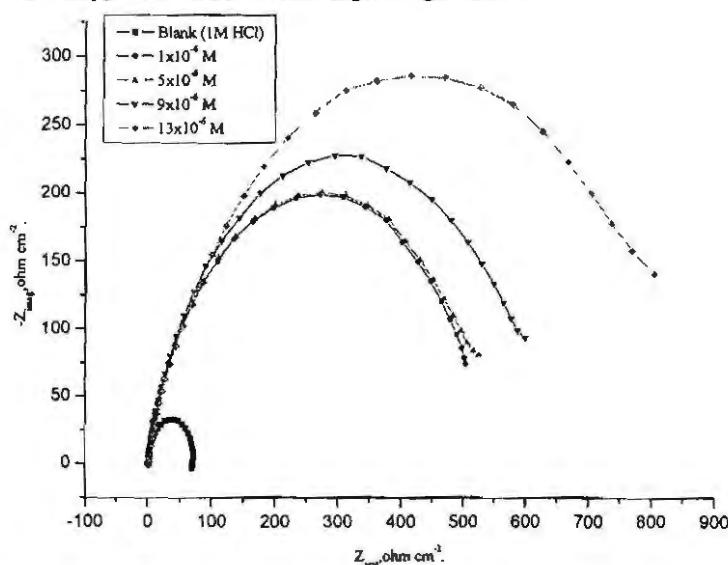
$$C_{dl} = (1/2\pi f \cdot R_{ct}) \quad (7)$$

The equivalent circuit that describes our metal/electrolyte interface is shown in Fig. (7) where R_s , R_{ct} and CPE refer to solution resistance, charge transfer resistance

and constant phase element, respectively. EIS parameters and % η were calculated and tabulated in Table (6). As we notice, Fig.(6) the impedance diagrams consists of one large capacitive loop. In fact, the presence of inhibitors enhances the value of R_{ct} in acidic solution indicating a charge-transfer process mainly controlling the corrosion of SS. The increase in R_{ct} values, and consequently of inhibition efficiency, may be due to the gradual replacement of water molecules by the adsorption of the inhibitor molecules on the metal surface to form an adherent film on the metal surface and this suggests that the coverage of the metal surface by the film decreases the double layer thickness. Values of double layer capacitance decrease to the maximum extent in the presence of inhibitors. This decrease of C_{dl} at the metal/solution interface with increasing the inhibitor concentration can result from a decrease in local dielectric constant which indicates that the inhibitors were adsorbed on the surface at both anodic and cathodic sites [E. McCafferty et al,(1972)].

Deviation of perfect circuit shape is often referred to the frequency dispersion of interfacial impedance. This anomalous phenomenon is generally attributed to the inhomogeneity of the metal surface arising from surface roughness or interfacial phenomena [H.Shin et al,(1989) and S.Martinez M.Metikos-Hukovic et al,(2003)].

The impedance data confirm the inhibition behavior of the inhibitors obtained with other techniques. From the data of Table (6), it can be seen that the j_{corr} values decrease significantly in the presence of these additives and the % η is greatly improved. The order of reduction in j_{corr} exactly correlates with that obtained from potentiostatic polarization studies. Moreover, the decrease in the values of j_{corr} follows the same order as that obtained for the values of C_{dl} . It can be concluded that the inhibition efficiency found from weight loss, polarization curves and electrochemical impedance spectroscopy measurements are in good agreement.



Fig(6): The Nyquist plots for 316L SS in 1 M HCl solution in the absence and presence of different concentrations of inhibitor (A) at 25 °C

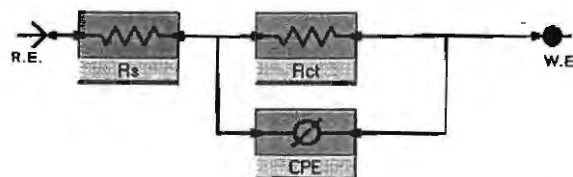


Figure (7) Electrical equivalent circuit used to fit the impedance data for 316L SS in 1 M HCl solution

Table (6) Electrochemical kinetic parameters obtained from EIS technique for the corrosion of 316L SS in 1 M HCl at different concentrations of investigated inhibitors at 25° C

compounds	Conc., M	$C_{dl} \times 10^{-6}$, $\mu\text{F cm}^{-2}$	R_{cu} , $\Omega \text{ cm}^2$	θ	% η
blank	0.0	14.0	72.2	----	----
A	1×10^{-6}	1.99	508.3	0.857	85.7
	5×10^{-6}	1.96	516.6	0.860	86.0
	9×10^{-6}	1.70	589.7	0.877	87.7
	13×10^{-6}	1.20	789.4	0.908	90.8
B	1×10^{-6}	3.00	335.7	0.785	78.5
	5×10^{-6}	2.80	348.8	0.793	79.3
	9×10^{-6}	2.40	406.7	0.822	82.2
	13×10^{-6}	1.90	532.7	0.864	86.4
C	1×10^{-6}	9.30	107.1	0.423	42.3
	5×10^{-6}	7.60	131.8	0.465	46.5
	9×10^{-6}	7.40	135	0.485	48.5
	13×10^{-6}	6.90	146.4	0.527	52.7

Electrochemical Frequency Modulation (EFM)

Several authors proposed electrochemical frequency modulation (EFM) as a new electrochemical technique for online corrosion monitoring [R.W. Bosch et al,(2001); K. F. Khaled et al,(2008); K.F.Khaled et al,(2005) and D. A. Jones et al,(1983)]. EFM is a rapid and nondestructive corrosion rate measurement technique that can directly give values of the corrosion current without prior knowledge of Tafel constants.

In corrosion research, it is known that the corrosion process is non-linear in nature, a potential distortion by one or more sine waves will generate responses at more frequencies than the frequencies of applied signal. Virtually no attention has been given

to the intermodulation or electrochemical frequency modulation. However, EFM showed that this non-linear response contains enough information about the corroding system so that the corrosion current can be calculated directly. The great strength of the EFM is the causality factors which serve as an internal check on the validity of the EFM measurement [Gamry,(2003)]. With the causality factors the experimental EFM data can be verified.

Figures (8-12) show the current response contains not only the input frequencies, but also contains frequency components which are the sum, difference, and multiples of the two input frequencies.

The larger peaks were used to calculate the corrosion current density (j_{corr}), the Tafel slopes (β_a and β_c) and the causality factors (CF-2 and CF-3). These electrochemical corrosion kinetic parameters at different concentrations of inhibitors in 1 M HCl at 25 °C were simultaneously determined and are listed in Table (7).

The inhibition efficiency % η calculated from Eq. (6), increases by increasing the studied inhibitor concentrations.

The causality factors CF-2 and CF-3 in Table (7) are close to their theoretical values of 2.0 and 3.0, respectively indicating that the measured data are of good quality.

The calculated inhibition efficiency obtained from weight loss, Tafel polarization and EIS measurements are in good agreement with that obtained from EFM measurements.

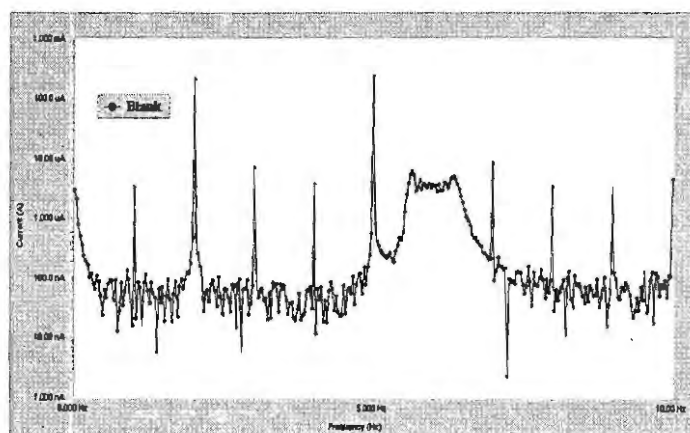


Figure (8) EFM spectra for 316L SS in 1 M HCl (blank)

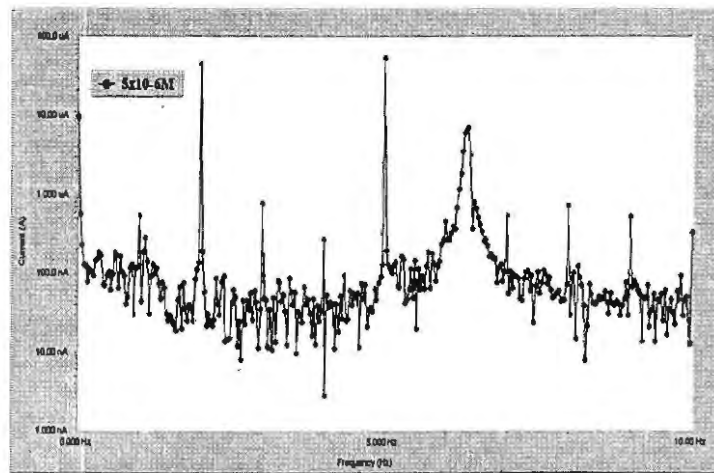


Figure (9) EFM spectra for 316 L SS in 1 M HCl in the presence of 5×10^{-6} M from inhibitor (A)

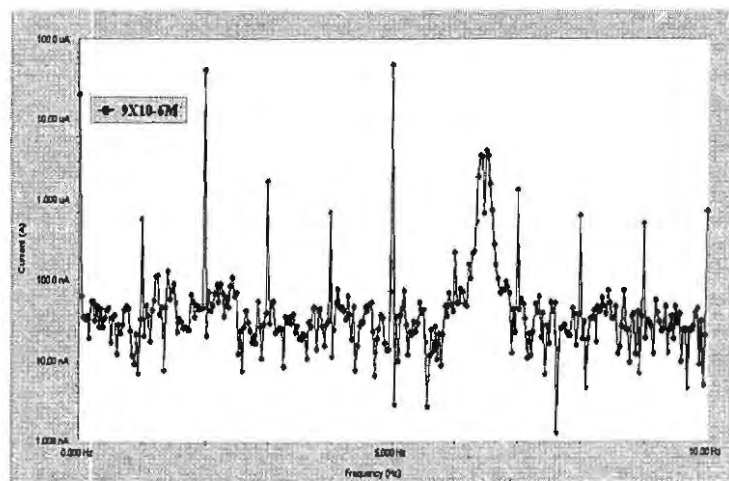
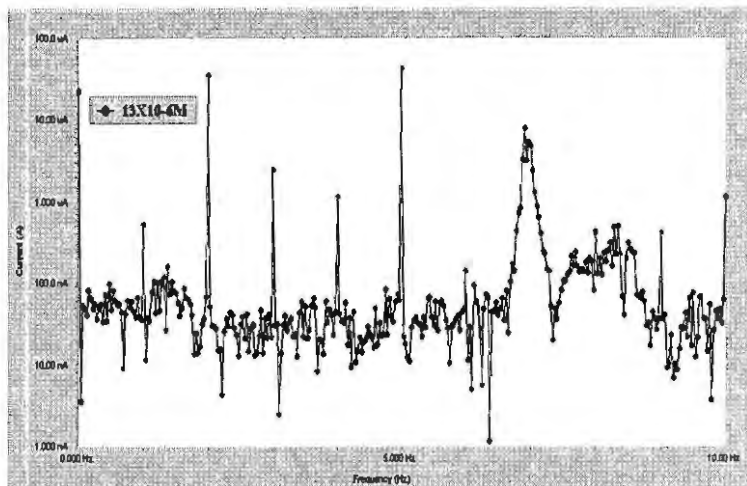


Figure (10) EFM spectra for 316 L SS in 1 M HCl in the presence of 9×10^{-6} M from inhibitor (A)



Figure(11) EFM spectra for 316 L SS in 1 M HCl in the presence of 13×10^{-6} M from inhibitor (A)

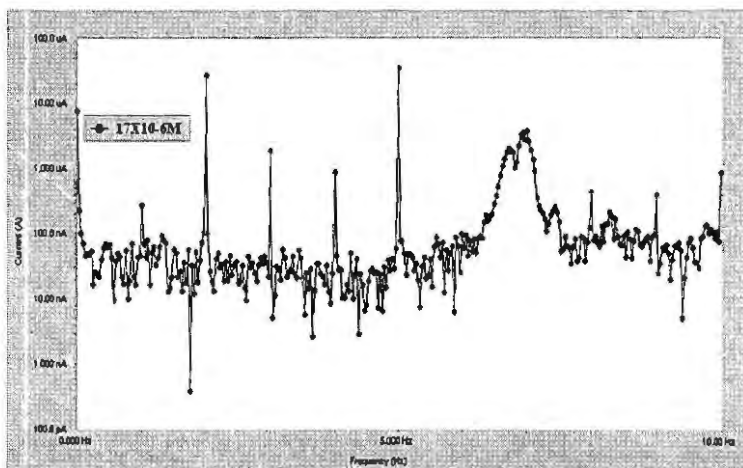


Figure (12) EFM spectra for 316 L SS in 1 M HCl in the presence of 17×10^{-6} M from inhibitor (A)

Table (7) Electrochemical kinetic parameters obtained from EFM technique for 316L SS in 1 M HCl in the absence and presence of different concentrations of investigated inhibitors

Inhibitor	Conc., M	$j_{corr.}$ $\mu A\ cm^{-2}$	β_a , mV dec^{-1}	β_c , mV dec^{-1}	CF-2	CF-3	% η_{EFM}
blank	1	342.00	88	108	1.9	2.9	-----
A	5×10^{-6}	75.20	94	102	2.1	2.8	78.0
	9×10^{-6}	73.53	96	119	2.1	2.7	78.5
	13×10^{-6}	73.37	92	198	2.0	2.9	78.3
	17×10^{-6}	62.40	93	189	2.0	3.0	81.8
B	5×10^{-6}	133.70	92	109	1.9	2.9	61.0
	9×10^{-6}	98.45	91	122	1.9	2.9	71.2
	13×10^{-6}	92.28	84	143	2.0	2.8	73.0
	17×10^{-6}	89.54	88	129	1.9	2.9	74.0
C	5×10^{-6}	201.00	90	105	1.8	2.8	42.0
	9×10^{-6}	196.60	90	104	2.0	2.7	42.5
	13×10^{-6}	183.80	93	107	2.0	2.7	46.3
	17×10^{-6}	171.70	91	107	2.1	2.8	50.0

CHEMICAL STRUCTURE AND CORROSION INHIBITION

Variation in structure of inhibitors molecules (A-C) takes place through the pyrazol-5-one derivatives. So, the inhibition efficiency will depends on this part of the molecule.

The weak dependence of the adsorption character of the reaction center of pyrazol-5-one derivatives on the electron density of the ring may be due to the centers of adsorption is not thoroughly conjugated to the ring.

In general, two modes of adsorption are considered on the metal surface in acid media. In the first mode, the neutral molecules may be adsorbed on the surface of carbon steel through the chemisorptions mechanism, involving the displacement of water molecules from the carbon steel surface and the sharing electrons between the hetero- atoms and iron. The inhibitor molecules can also adsorb on the carbon steel surface on the basis of donor-acceptor interactions between π -electrons of the aromatic ring and vacant d-orbitals of surface iron atoms. In the second mode, since it is well known that the steel surface bears positive charge in acid solution [G.N. Mu et al,(1996) and A.K. Singh et al,(2010)], so it is difficult for the protonated molecules to approach the positively charged carbon steel surface due to the electrostatic repulsion. Since chloride ions have a smaller degree of hydration, thus they could bring excess negative charges in the vicinity of the interface and favor more adsorption of the positively charged inhibitor molecules, the protonated pyrazol-5-one derivatives adsorb

through electrostatic interactions between the positively charged molecules and the negatively charged metal surface. Thus there is a synergism between adsorbed Cl^- ions and protonated pyrazol-5-one derivatives. Thus we can conclude that inhibition of carbon steel corrosion in 2 M HCl is mainly due to electrostatic interaction. The decrease in the inhibition efficiency with rise in temperature supports electrostatic interaction.

Inhibitor (A) is the most efficient inhibitor because of: i) the presence $m\text{-OCH}_3$ group ($\sigma = -0.12$) which enhances the delocalized π -electrons on the molecule ii) also may add an additional active center to the molecule due to its oxygen atom and also iii) due to its higher molecular size. Inhibitor (B) comes after compound (A) in inhibition efficiency, because the presence of $m\text{-CH}_3$ with ($\sigma = -0.07$) which contribute less electron density to the molecule. Inhibitor (C) is the least efficient inhibitor. This may be due to: i) Its highest electrophilic character ($\sigma_{\text{NO}_2} = +0.78$) of NO_2 group ii) NO_2 may reduced easily in acid medium and iii) the evolved heat of hydrogenation may aids desorption of the molecules. According, the previous discussion, the nature of substituted group, whether electron donating or withdrawing reflects its effect on the inhibition efficiency.

CONCLUSIONS

The investigated compounds show excellent performance as corrosion inhibitors in HCl solution. The inhibition efficiency of pyrazol-5-one derivatives follows the order: $A > B > C$. Polarization studies showed that pyrazol-5-one derivatives behave as mixed type inhibitors for SS in HCl solution. Impedance studies indicated that R_{ct} values increased, while C_{dl} values decreased in the presence of the inhibitors. The adsorption of the investigated inhibitors was found to follow the Temkin adsorption isotherm indicating that the inhibition process occurs via adsorption. The % η obtained from weight loss, polarization curves, electrochemical impedance spectroscopy and electrochemical frequency modulation are in good agreement.

REFERENCES

- A. Atrens, B. Baroux, M. Mantel, *J. Electrochem. Soc.*, 144 (1997) 3697.
- A.K. Singh and M.A. Quraishi, *Corros. Sci.*, 52 (2010) 1529.
- A. Popova, E. Sokolova, S. Raicheva, M. Christov, *Corros. Sci.*, 45 (2003) 33.
- A.S. Fouada, G.Y. Elewady, A. El-Askalani, K. Shalaby, *Zastita Materijala*, 51(4) (2010) 205-219.
- Atia and M. M. Saleh. *J. Appl. Electrochem.*, 33(2) (2003) 171.
- C.D. Dillon, *Performance*, 33 (1994) 62.
- D. A. Jones, *Principles and Prevention of Corrosion*, second ed., Prentice Hall, Upper Saddle River, NJ, 1983.
- D. A. Jones, *Principles and Prevention of Corrosion*, second ed., Prentice Hall, Upper Saddle River, NJ, 1983.
- E.E. Oguzie, *Mater. Chem. Phys.*, 99 (2006) 441-446.
- E. Kamis, F. Bellucci, R.M. Latanision, E.S. El-Ashry, *Corrosion*, 47 (1991) 677.
- E. McCafferty, N. Hackerman, *J. Electrochem. Soc.* 119 (1972) 146.
- A.H. Fadda, A. Zaki, Kh. Samir and F. A. Amsr, *Khim. Geterotsiki Soedin (J; Chemistry of Heterocyclic Compounds)*, 9 (2003) 1413-1419
- E. McCafferty, N. Hackerman, *J. Electrochem. Soc.* 119 (1972) 146.
- F. Mansfeld, *Electrochim. Acta*, 35 (1990) 1533.
- F.M. Donahue, K. Noor, *J. Electrochem. Soc.*, 112 (1965) 886.
- F. Mansfeld, M. W. Kendig, S. Tsai, *Corrosion*, 38 (1982) 570.
- Gamry Echem Analyst Manual, 2003.
- G.N. Mu, T.P. Zhao, M. Liu and T. Gu, *Corrosion*, 52 (1996) 853.
- H. Shin, H. Mansfeld, *Corros. Sci.*, 29 (1989) 1235.
- I.O'MBockris, D.A. Swinkles, *J. Electrochem. Soc.*, 111 (1964) 736.
- K.C. Emergul, M. Hayvalf, *Corros. Sci.*, 48 (2006) 797-812.
- K. F. Khaled, *Int. J. Electrochem. Sci.*, 3 (2005) 462.

K. F. Khaled, *Electrochim. Acta*, 53 (2008) 3484.

M.A.Amin, S.S.Abd El-Rehim, M.M.El-Naggar, H.T.Abd El-Fattah, *J.Mater.Sci.*, 44 (2009) 6258.

M. Kendig, S. Jeanjaquet, *J. Electrochem. Soc.*, 149 (2002) B47.

M. T. Said, S. A. Ali and S. U. Rahman. *Anti-Corros. Meth. Mater.*, 50(3) (2003) 201.

P.Q.Zhang, J.X.Wu, W.Q.Zhang, X.Y.Lu, K.Wang, *Corros.Sci.*, 34 (1993) 1343.

R. W. Bosch, J. Hubrecht, W. F. Bogaerts, B. C. Syrett, *Corrosion*, 57 (2001) 60.

S.Martinez M.Metikos-Hukovic, *J. Appl. Electrochem.*, 33 (2003)1137.

S. Tamilselvi and S. Rajeswari. *Anti-Corrosi. Meth.Mater.*, 50(3) (2003) 223.

W. Huilong, Z. Jiashen and L. Jing. *Anti-Corros. Meth.Mater*, 9(2) (2002) 127.

W.P.Wang, D.Casta, P.Marcus, *J.Electrochem;Soc.*, 141 (1994) 2669

الملخص العربي

دور بعض مشتقات بيرزول -5-ون كمثبطات تاكل الصلب المقاوم 316L في محلول 1 مولار من حامض الهيدروكلوريك

عبد العزيز فودة *، غادة العواضي، سارة فتحى
قسم الكيمياء، كلية العلوم ، جامعة المنصورة ، مصر

الصلب المقاوم 316L من اهم انواع الصلب التى تستخدم فى محطات الكهرباء لكونها تواجه مشكلة التاكل فى وجود حامض الهيدروكلوريك وهذا البحث يناقش كيفية حماية الصلب المقاوم باستخدام بعض مشتقات بيرزول - 5-ون وتم مناقشة قدرة وكفاءة بعض مشتقات بيرزول-5-اون على تثبيط تاكل الصلب المقاوم 316L باستخدام الطرق الكيميائية (طريقة الفقد فى الوزن) وايضا الطرق الكهروكيميائية (طريقة الاستقطاب الكهربي وايضا طريقة المانعة الامبكتروسكوبية) . اظهرت النتائج ان هذه المركبات تعمل كمثبطات جيدة وتم دراسة تأثير درجة الحرارة ووجد ايضا ان امتزاز هذه المركبات على سطح الصلب المقاوم يتبع ايزوثيرم* تمكن*